ELSEVIER

Journal of Quantitative Spectroscopy & Radiative Transfer 93 (2005) 337–348

Journal of Quantitative Spectroscopy & Radiative Transfer

www.elsevier.com/locate/jqsrt

Temporal analysis of reflected optical signals for short pulse laser interaction with nonhomogeneous tissue phantoms

Ashish Trivedi, Soumyadipta Basu, Kunal Mitra*

Mechanical and Aerospace Engineering Department, Florida Institute of Technology, 150 W University Boulevard, Melbourne, FL, 32901, USA

Received 1 February 2004; accepted 1 July 2004

Abstract

The use of short pulse laser for minimally invasive detection scheme has become an indispensable tool in the technological arsenal of modern medicine and biomedical engineering. In this work, a time-resolved technique has been used to detect tumors/inhomogeneities in tissues by measuring transmitted and reflected scattered temporal optical signals when a short pulse laser source is incident on tissue phantoms. A parametric study involving different scattering and absorption coefficients of tissue phantoms and inhomogeneities, size of inhomogeneity as well as the detector position is performed. The experimental measurements are validated with a numerical solution of the transient radiative transport equation obtained by using discrete ordinates method. Thus, both simultaneous experimental and numerical studies are critical for predicting the optical properties of tissues and inhomogeneities from temporal scattered optical signal measurements.

Keywords: Short pulse laser; Transient radiative transfer; Biomedical imaging; Scattering media

1. Introduction

Optical imaging has attracted significant interest as a potential noninvasive diagnostic tool for detecting tumors and other abnormalities hidden in biological tissues. For this purpose, various

*Corresponding author. Tel.: +1 321 674 7131; fax: +1 321 674 8813
E-mail address: kmitra@fit.edu (K. Mitra).

0022-4073/$ - see front matter © 2004 Elsevier Ltd. All rights reserved.
doi:10.1016/j.jqsrt.2004.08.033

Nomenclature

c	speed of light
I	scattered diffused intensity
k_a, k_e, k_s	absorption, extinction and scattering coefficient
P_n	Legendre polynomials
S	source function
t	time
t_p	pulse width
w_m	weight
x, y	spatial coordinates
Φ	scattering phase function
Θ	scattering angle
Ω_μ	propagation direction
δ	Dirac delta function
μ, η, ξ	direction cosines

optical techniques such as frequency-resolved [1], time-resolved [2] and CW techniques have been proposed that use different geometries [3]. These techniques offer several advantages often not available in established imaging methods such as ultrasound, X-ray computed tomography and magnetic resonance imaging [4]. This is due to the fact that visible light is nonionizing over many wavelengths and is known to function well for medical probes. In particular, red and infrared light pass relatively easily through such structures as the skull, brain and breast due to lesser absorption and scattering and is well tolerated in large doses. Visible light can, therefore, be used to quantify tissue properties. Visible and near-infrared optical tomography has been recognized as an ideal noninvasive diagnostic technique due to its potential low-cost and minimal side-effects [2,3]. Optical tomography is capable of functional imaging and is a particularly interesting technique because it provides cross-sectional views of physiological processes not obtainable with other methods. Since light cannot penetrate more than a few millimeters of tissue without being scattered a large number of times, if optical imaging is to become a viable diagnostic technique, it must rely exclusively on information encoded in scattered light [5].

When a tissue is illuminated with a short pulse of light, the reflected/transmitted pulse is significantly broadened due to multiple scattering in the media. The scattered signals from the tissue can be used to generate information about the tissue interior. Researchers have approached the task of imaging in two ways, using time-resolved measurements or the frequency-domain equivalent. Frequency-domain methods involve harmonically modulated photon density waves and phase-resolved detection, which measures the phase shift of the photon density waves, while the time-resolved methods use pulsed excitation and gated detection to examine the response of tissue to incident pulsed light sources [6].

This work has been motivated by a number of potential clinical applications specially as a safer alternative to X-rays and as a means of detecting tumors. The scattered signals from tissue phantoms can be used to generate images with significantly better spatial resolution [7]. The image

reconstruction method depends on developing a forward model for simulating boundary measurements for a given experimental setup and known optical tissue parameters and using it to determine the tissue parameters from a given experimental setup and a given set of measurements [7–9]. In this work, a time-resolved technique has been used to detect tumors in the tissues using transmitted/reflected temporal signals due to an incident short-pulse laser source. In optical tomography involving a short-pulse laser, the short-pulse laser source is focused on the region to be probed and the time-dependent scattered reflected and transmitted signals are measured at different locations using ultrafast detectors. Short-pulse laser probing techniques for diagnostics have distinct advantages over very large pulse width or continuous wave lasers primarily due to the additional information conveyed by the temporal distribution of the observed signal. The distinct feature is the multiple-scattering-induced temporal distributions, which persists for a time period greater than the duration of the source pulse and is a function of the source pulse width as well as the optical properties of the medium. If the detection is carried out at the same short time-scale (comparable to the order of the pulse width), the signal continues to be observed even at large times after the pulse has been off, due to the time taken for the photons to migrate to the detector after multiple scattering in the media. On the other hand, when conventional CW laser sources are utilized, the information available is the magnitude of the net attenuation and the angular distribution of the transmitted or reflected signal, which does not provide useful information about medium properties.

Several other techniques that have been previously used for biomedical imaging focus on the initial transients of the temporal signal. Time gating, optical coherence interferometry techniques and streak camera applications have been used for evaluating the earliest arriving photons [10]. However, these ballistic components may not be of practical use for tissues thicker than a few centimeters because they are not measurable with increasing tissue thickness. The frequency-domain techniques developed for biomedical imaging also suffer from low resolution due to nonavailability of high-frequency source restricting the temporal resolution to a few nanoseconds.

One of the objectives of this work is to validate the forward solutions of transient radiative transport equation necessary to analyze short-pulse laser propagation through tissues. In most of the earlier analyses, the transient term of the radiative transport equation (RTE) is usually neglected. This assumption does not lead to errors, as the temporal variations of observed signals are slow compared to the time of flight of a photon. However, in applications involving short-pulse laser interactions with tissues, the transient term effect must be considered in the RTE [11]. Transient solution of radiative transfer equation for one-dimensional geometry for the case of short-pulse laser incidence has been developed and reported in the literature [11]. The work has been extended to two-dimensional geometry using the simplified first-order spherical harmonics (P_1) approximation for a rectangular geometry [12]. Integral equation formulation techniques for the transient radiative transport equation have been also developed [13]. However, the P_1 model underestimates the speed of light propagation and the integral formulation is difficult to apply to complex geometries. The Monte Carlo (MC) method has also been used by many researchers [14]. But the MC method requires a large number of emitted bundles to obtain smooth accurate solutions, particularly for optically thick samples, and is computationally expensive [15]. Radiation element method with ray tracing model has been also developed for solution of transient radiative transfer equation [16]. The discrete ordinate method (DOM) has become popular for solving transient radiative transport equation accurately and efficiently. The

one-dimensional DOM has been used to analyze short-pulse laser propagation through scattering-absorbing media such as tissues, and ocean water [11,17].

In this paper, the experimentally measured temporal reflected optical signals from a tissue phantom containing inhomogeneities due to short-pulse laser irradiation having a Gaussian distribution are compared with the numerical solutions of transient radiative transport equation. The DOM, in conjunction with the piecewise parabolic method scheme developed previously by the authors, is used to obtain numerical solutions [18]. The analysis of temporal reflected optical signals as performed in this paper is important for most of the biomedical imaging and probing applications involving detection of tumors in tissues. Such studies are critical for predicting the optical properties of tissues and inhomogeneities/tumors as well as the location and size of the tumor/inhomogeneity. The temporal optical reflected signals from tissue phantoms containing inhomogeneities/tumors imbedded in it are collected using fiber-optic collimator lens assembly and connected at the other end to the streak camera. A parametric study involving different scattering and absorption coefficients of tissue phantoms and inhomogeneities, detector position, as well as the inhomogeneity size is performed. The authors have previously performed a study for experimental validation of transmitted optical signals for the case of a square pulse [19]. In those measurements, the transmitted signal is captured by the focusing lens of the streak camera, unlike the fiber-optic approach as used in this paper. Some modeling and experimental results of the transmitted optical signals for the case of short-pulse laser source having a Gaussian distribution are also presented.

2. Experimental procedure

Fig. 1 shows the schematic of the experimental setup. The laser beam from an argon-ion mode locked laser having a pulse width (t_p) = 200 ps at FWHM operating at a frequency of 76 MHz and having a wavelength of 514 nm is split into two parts. One is used as the time reference and the other is incident on the tissue phantom. A translation stage is introduced for an adjustable optical delay in the reference beam to be used as marker for the determination of the origin of the time scale. The beam is incident on the phantom and scattered transmitted or reflected signals are

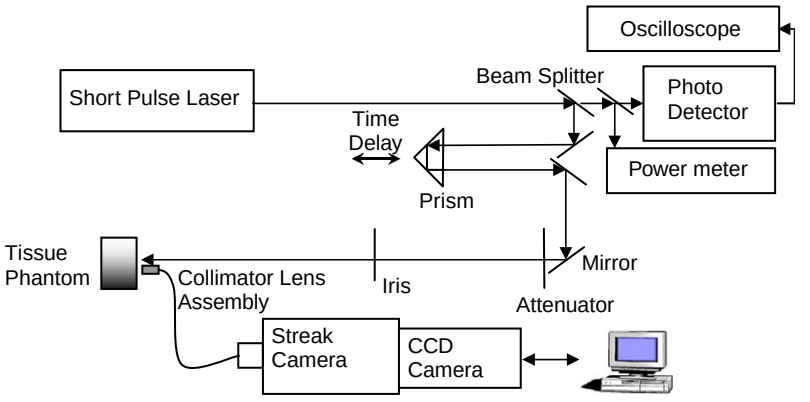

Fig. 1. Schematic of the experimental setup.

collected into a Hamamatsu streak camera unit using a collimator lens assembly. The streak unit comprises ultra fast synchroscan unit with the frequency-tuning unit, coupled with a Hamamatsu CCD camera. The time resolution of streak camera used in this study is 10 ps. The streak camera image acquisition control is remotely done using the HPDTA_32 software, which is also used for image processing. An image integration technique is used for collection of data, which helps to clearly distinguish noise from useful data for low-intensity optical signals. The streak camera is triggered from the mode locker at the rate of 76 MHz. Detailed discussion of the experimental procedure can be found in the literature [19].

3. Mathematical formulation

In this paper, the tissue medium is approximated by an anisotropically scattering and absorbing rectangular enclosure in which an inhomogeneity is imbedded (see Fig. 2). The transient radiative transfer equation (RTE) is given by [11,20]

$$\frac{1}{c}\frac{\partial I(x,y,\Omega,t)}{\partial t}+\mu\frac{\partial I(x,y,\Omega,t)}{\partial x}+\eta\frac{\partial I(x,y,\Omega,t)}{\partial y}+k_e I(x,y,\Omega,t)=\frac{k_s}{4\pi}\int_{4\pi}\Phi(\Omega',\Omega)I(x,y,\Omega',t)\,d\Omega' + S(x,y,\Omega,t), \quad (1)$$

where I is the scattered diffuse intensity ($W\,m^{-2}\,sr^{-1}$), k_e and k_s are the extinction coefficient, and the scattering coefficient, respectively, Φ is the phase function, Ω is the solid angle, c is the velocity of light in the medium, x and y are the spatial coordinates, t is the time and S is the source term. The scattering phase function can be represented in a series of Legendre polynomials P_n by

$$\Phi(\Omega',\Omega)=\sum_{n=0}^{N}(2n+1)g^n P_n[\cos(\Theta)], \quad (2a)$$

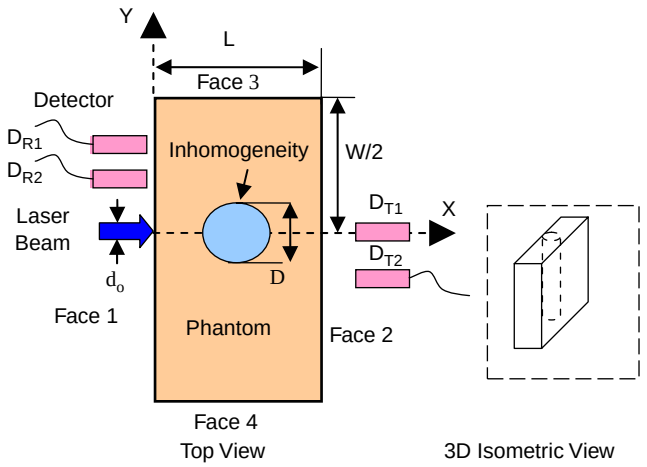

Fig. 2. Schematic of a tissue phantom containing inhomogeneity.

where g is the asymmetry factor and N is the anisotropy factor. Higher the value of g and N, more forward scattered is the phase function of the media. Tissues usually are highly forward scattered media. Typical values of g vary from 0.75 to 0.9 [18,21,22] and N varies from 12 to 20. The scattering angle Θ is represented by

$$\cos(\Theta) = \mu\mu' + \eta\eta' + \xi\xi', \tag{2b}$$

where μ, η and ξ are the directions cosines of the light propagation direction Ω.

The pulsed radiation incident on the tissue medium at face 1 (see Fig. 2) is a Gaussian pulse having a temporal duration (pulse width) t_p at full-width half-maximum (FWHM). The intensity can be separated into a collimated component, corresponding to the incident source and a scattered intensity. If I_c is the collimated intensity, then I is the remaining intensity described by Eq. (1). The collimated component of the intensity for a Gaussian laser pulse source is represented by

$$I_c(x, y, \Omega, t) = I_0 \exp[-k_a x - 2.77(t/t_p)^2] \exp(-y^2/\sigma^2)\delta(\Omega - \Omega_0), \tag{3}$$

where I_0 is the intensity leaving the wall towards the medium, $\delta(t)$ the Dirac delta function and $\sigma^2/2$ is the spatial variance of the Gaussian laser beam. The source function S formed from the collimated irradiation is then given by

$$S(x, y, \Omega, t) = \frac{k_s}{4\pi} \int_{4\pi} \Phi(\Omega', \Omega) I_c(x, y, \Omega', t)\, d\Omega'. \tag{4}$$

The boundary conditions are such that the intensity leaving the boundary surface is composed of the contribution of the outgoing emitted intensity and the reflection of incoming radiation in direction Ω. The refractive indices of the base tissue phantom and inhomogeneities are chosen to be the same; then the laser beam does not change direction after entering the inhomogeneity. In the discrete ordinates method, the RTE and the associated boundary condition are replaced with a set of equations for a finite number of M directions that cover 4π sr solid angles. The integral terms of Eqs. (1) and (4) are reformulated with the aid of an angular quadrature of order M. The discrete form of the time-dependent radiative transport equation in the direction Ω_m is then represented as

$$\frac{1}{c}\frac{\partial I_m(x, y, t)}{\partial t} + \mu_m \frac{\partial I_m(x, y, t)}{\partial x} + \eta_m \frac{\partial I_m(x, y, t)}{\partial y} = -k_e I_m(x, y, t) + \frac{k_s}{4\pi} \sum_{m'=1}^{M} w_{m'} \Phi_{m'm} I_{m'}(x, y, t) + S_m(x, y, t), \tag{5}$$

where $m = -M, \ldots, -1, 1, \ldots, M, \{\Omega_m, w_m\}$ defines a quadrature of M discrete directions Ω_m to which the weights w_m are associated. Details of this solution methodology can be found in [18].

4. Results and discussions

Reflected and transmitted signals from tissue phantoms with and without inhomogeneity are measured experimentally. Numerical simulation results obtained by solving two-dimensional RTE using discrete ordinate method have been used to validate the experimental measurements. The tissue phantoms used are cast by mixing araldite resin having a refractive index (n) of 1.54 together with an anhydride and a hardener. Typical sample cross-section used is 25 mm × 50 mm

with varying thickness of 8 and 12 mm. Titanium dioxide (TiO_2) particles having a mean diameter of 0.3 μm are added as scatterers and dye is used as an absorber. The scattering and absorption coefficients are varied by varying the concentration of TiO_2 and dye in the resin matrix. Inhomogeneities typically of 4 mm diameter are drilled in the samples and filled with different scattering and absorption coefficients than the base resin matrix [23]. Details about phantom preparation can be found in the literature [19].

A typical experimental measurement scheme is shown in Fig. 2, where the reflected signals are collected by fiber-optic collimator lens assembly (detector) at positions D_{R1} and D_{R2} while the transmitted signals are measured at positions D_{T1} and D_{T2}. It should be noted from Fig. 2 that the transmitted signals can be collected at the beam axis, while the reflected signals are always collected off-axis to avoid interference with the incident beam. Fig. 3 shows the comparison of transmitted signals at position D_{T1} between numerical model and experimental measurements for a homogeneous tissue phantom having thickness $L = 8\,\text{mm}$, $k_s = 10\,\text{mm}^{-1}$ and $k_a = 0.005\,\text{mm}^{-1}$. A good agreement between the modeling result and experimental measurements is obtained within the uncertainty limits of the streak camera, which is ± 10 ps. Similar comparison for temporal reflected signals for the same homogenous tissue phantom is shown in Fig. 4. These experiments have been performed for two positions of the collimator detector. It is observed that the temporal spread of the scattered signal increases as the collimator lens assembly moves away from the beam. This is due to a larger optical path being traveled by photons in the medium.

Fig. 5 shows comparison of temporal measured reflected signals obtained for a tissue phantom containing inhomogeneity with that of the numerical model. The collimator lens assembly is placed 3.5 mm from the laser beam axis. The properties of the tissue phantom used are $k_s = 10\,\text{mm}^{-1}$ and $k_a = 0.005\,\text{mm}^{-1}$ and for inhomogeneity/tumor properties values used are $k_s = 20\,\text{mm}^{-1}$ and $k_a = 0.005\,\text{mm}^{-1}$. Fig. 6 shows corresponding spatial intensity profiles obtained by performing a line scan along face 1 for different times. During the line scan, the collimator lens assembly and the mirror in which the laser beam is incident are mounted on a translation stage and move along face 1 as shown in Fig. 2. The demarcation between the tissue phantom and the inhomogeneity is most prominent at 315 ps as evident from Fig. 6. This demarcation is not evident

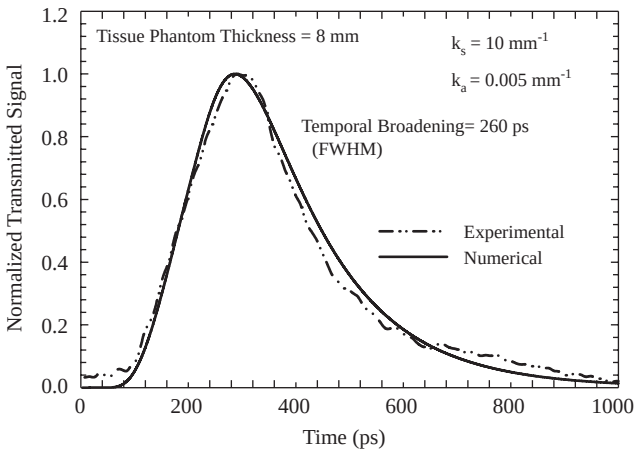

Fig. 3. Comparison of temporal transmitted signal for a homogenous tissue phantom.

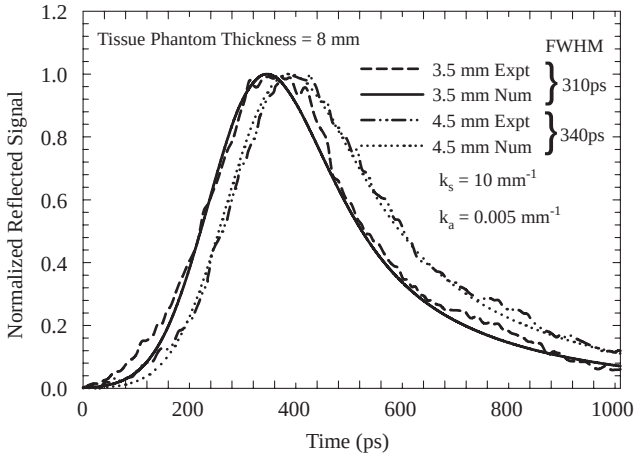

Fig. 4. Comparison of temporal reflected signals for a homogeneous tissue phantom for different detector positions with respect to the laser beam.

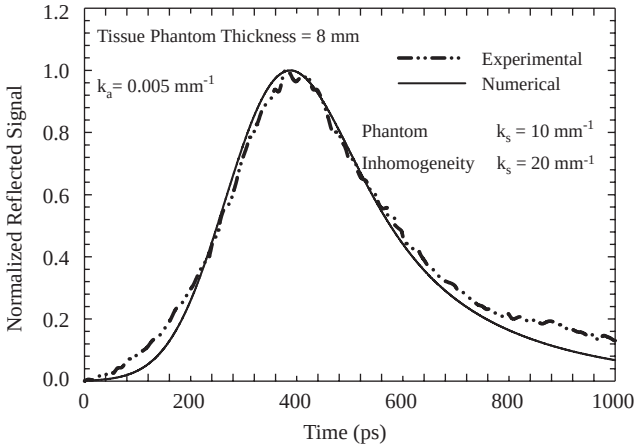

Fig. 5. Comparison of temporal reflected signal for a tissue phantom containing inhomogeneity.

at larger times as well as at smaller times. Hence, this method can be developed into an effective technique to detect inhomogeneity/tumor location in tissues. Spatial reflected and transmitted optical signals obtained by line scan are validated with the numerical model for a particular time instant as shown in Fig. 7. For measurements in transmission mode line scanning is performed along face 2 as shown in Fig. 2. It is interesting to note that the time instant chosen in Fig. 7 corresponds to the time when the demarcation is most prominent for both transmission and reflection measurements. Also, a change in intensity magnitude and distribution is observed for the transmitted and reflected optical signals. There is an excellent matching between the experimental measurements and numerical models as evident in Fig. 7. In Fig. 8 the scattering coefficient of the phantom has been varied, keeping the inhomogeneity of optical properties constant. It can be observed that as the difference between the scattering properties of the

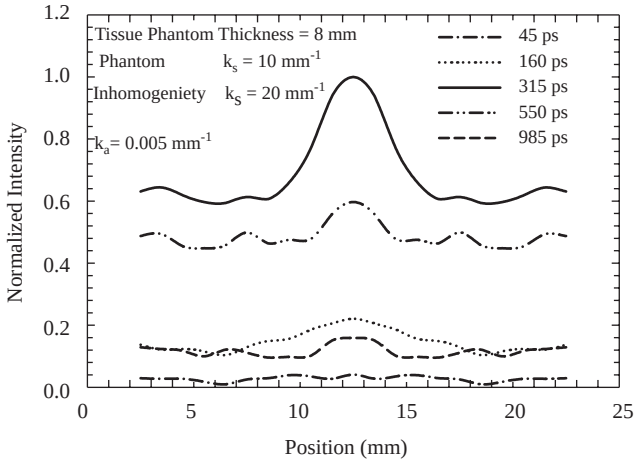

Fig. 6. Experimentally measured spatial intensity distribution in a tissue phantom containing inhomogeneity.

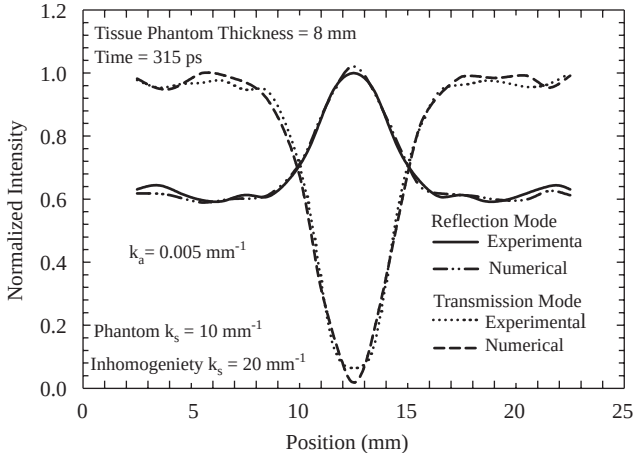

Fig. 7. Comparison of spatial intensity distribution in a tissue phantom containing inhomogeneity for measurements in transmission and reflection modes.

phantom and inhomogeneity increases, a better contrast is obtained about the inhomogeneity location, thus making it easier to locate the inhomogeneity.

Fig. 9 shows the effect of variation of inhomogeneity size obtained both numerically and experimentally for a 12-mm thick tissue phantom. As inhomogeneity size increases, light undergoes more scattering in the inhomogeneity, thus broadening the pulse. A shift in the peak in the temporal axis also contains qualitative information about the inhomogeneity size. The case of homogeneous phantom is also plotted in Fig. 9 to demonstrate the effect of temporal broadening and shift due to the presence of inhomogeneities.

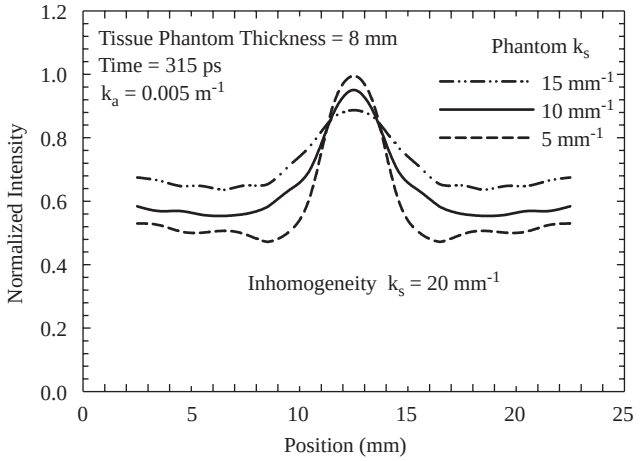

Fig. 8. Experimentally measured spatial intensity distribution for various scattering coefficients of the tissue phantom keeping the inhomogeneity of optical properties constant.

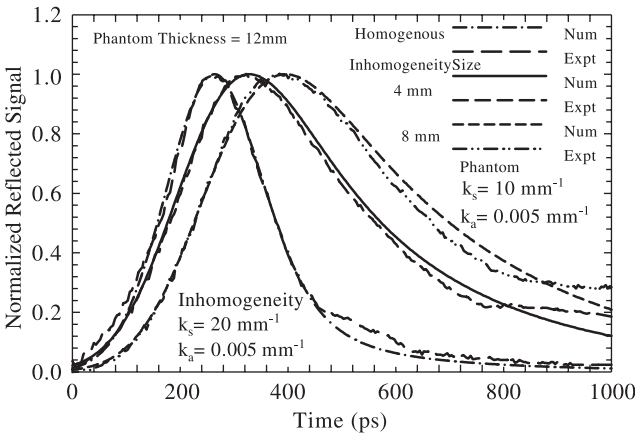

Fig. 9. Effect of inhomogeneity size variation on reflected signals for a tissue phantom containing inhomogeneity.

5. Conclusion

An extensive experimental study, validated by a numerical model, has been performed to investigate the scattering of light in tissue media containing inhomogeneity/tumor. Both the reflected and transmitted optical signals can be used to obtain information about inhomogeneity embedded in the tissue. Parametric study as performed in this work demonstrates that it is possible to differentiate between healthy tissue and tumors/inhomogeneities using time-resolved analysis. Accurate validation of the forward transient radiative transport equation with the experimentally measured data is critical before the development of the inverse algorithms. Short-pulse laser probing is a nascent technology and this work for detection of tumors in tissues can be furthered by experiments on animal models.

Acknowledgments

The authors acknowledge support from Florida Department of Health and Florida Photonics Center of Excellence.

References

[1] Fantini S, Walker SA, Franceschini MA, Moesta K, Schlag T, Kaschke M, Gratton E. Assessment of the size, position, and optical properties of breast tumors in vivo by non-invasive optical methods. Appl Opt 1998;37:1982–9.
[2] Hebden JC, Schmidt FEW, Fry ME, Schweiger M, Hillman EMC, Delpy DT, Arridge SR. Simultaneous reconstruction of absorption and scattering images by multichannel measurement of purely temporal data. Opt Lett 1999;24:534–6.
[3] Siegel AM, Marota JJA, Boas DA. Design and evaluation of a continuous-wave diffuse optical tomography system. Opt Exp 1999;4:287–98.
[4] Pfefer TJ, Bennett SLM, Gall CL, Wilke JA, Durkin AJ, Ediger MN. Reflectance-based determination of optical properties in highly attenuating tissue. J Biomed Opt 2003;8:206–15.
[5] Rinneberg H, Grosenick D, Wabnitz H, Danlewski H, Moesta K, Schlag P. Time-domain optical mammography: results on phantoms, healthy volunteers, and patients. Advances in Optical Imaging and Photon Migration. OSA Trends in Optics and Photonics. Optical Society of America Orlando, 1998. p.278–80.
[6] Prahl SA, Van Gemert MJC, Welch AJ. Determining the optical properties of turbid media by using adding–doubling method. Appl Opt 1993;32:559–68.
[7] Hebden JC, Veenstra H, Dehghani H, Hillman EMC, Schweiger M, Arridge SR, Delpy DT. Three dimensional time-resolved optical tomography of a conical breast phantom. Appl Opt 2001;40:3278–87.
[8] Marion JE, Kim BM. Medical applications of ultra-short-pulse lasers. SPIE—Commercial and Biomedical Applications of Ultrafast Lasers, 1999. p.42–50.
[9] Kurtz R.M, Elner V, Liu TX, Juhasz FH, Loesel C, Horvath M, Niemz H, Noack F. Plasma-mediated ablation of biological tissue with picosecond and femtosecond laser pulses. SPIE Proceedings, 1997. p.192–200.
[10] Zaccanti G, Hebden J, Sassaroli A, Blumetti C, Bassani M, Ismaelli A. Imaging of scattering inhomogeneities within highly diffusing media. Proceedings of SPIE—The International Society for Optical Engineering, 1997. p. 462–70.
[11] Mitra K, Kumar S. Development and comparison of models for light pulse transport through scattering absorbing media. Appl Opt 1999;38:188–96.
[12] Mitra K, Lai M, Kumar S. Two-dimensional transient radiative transport in participating media within a rectangular enclosure. AIAA J. Thermophys Heat Transfer 1997;11:409–14.
[13] Tan ZM, Hsu PF. An integral formulation of transient radiative transfer. ASME J. Heat Transfer 2001;123:466–75.
[14] Sawetprawichkul A, Hsu PF, Mitra K, Sakami MA. Monte Carlo study of the transient radiative transfer within the one-dimensional multi-layered slab. International Mechanical Engineering Congress and Symposium, 2000. p. 145–53.
[15] Guo Z, Aber J, Garetz BA, Kumar S. Monte carlo simulation and experiments of pulsed radiative transfer. JQSRT 2002;73:159–68.
[16] Guo Z, Kumar S. Radiation element method for transient hyperbolic radiative transfer in plane parallel inhomogeneous media. Numer Heat Transfer: Part B 2001;39:371–87.
[17] Mitra K, Churnside JH. Transient radiative transfer equation applied to oceanographic lidar. Appl Opt 1999;38:889–95.
[18] Sakami M, Mitra K, Hsu PF. Analysis of light-pulse transport through two-dimensional scattering-absorbing media. JQSRT 2002;73:169–79.

[19] Das C, Trivedi A, Mitra K, Vo-Dinh T. Experimental and numerical analysis of short-pulse laser interaction with tissue phantoms containing inhomogeneities. Appl Opt 2003;42:5173–80.
[20] Ishimaru A. Diffusion of light in turbid material. Appl Opt 1989;28:2210–5.
[21] Tromberg BJ, Svaasand LO, Tsay T, Haskell RC. Properties of photon density waves in multiple-scattering media. Appl Opt 1993;32:607–13.
[22] Jarlman O, Berg R, Andersson-Engels S, Svanberg S, Pettersson H. Time-resolved white light transillumination for optical imaging. Acta Radiol 1997;38:185–9.
[23] Firbank M, Delpy DT. A design for a stable and reproducible phantom for use in near infra-red imaging and spectroscopy. Phys Med Biol 1993;38:847–53.